

6.2 HIGH-RESOLUTION LARGE-EDDY SIMULATIONS OF THE RIVIERA VALLEY: METHODOLOGY AND SENSITIVITY STUDIES

Fotini Katopodes Chow^{1*}, Andreas P. Weigel², Robert L. Street¹, Mathias W. Rotach^{2,3}, and Ming Xue⁴

¹Environmental Fluid Mechanics Laboratory, Stanford University, Stanford, California

²Institute for Atmospheric and Climate Science, ETH, Zurich, Switzerland

³Swiss Federal Office for Meteorology and Climatology, MeteoSwiss, Zurich, Switzerland

⁴School of Meteorology and Center for Analysis and Prediction of Storms, University of Oklahoma

1. INTRODUCTION

High-resolution simulations of the atmospheric boundary layer have recently become possible due to increases in available computational power; however, the influence of parameterizations such as those for turbulence, land surface conditions and radiative forcing, the configuration of initial conditions, lateral boundary conditions, and the choice of numerical grids is highly situation dependent. Simulations are generally performed using "the best available" information and datasets. The situation is further complicated in the case of highly complex terrain such as the European Alps, because the numerical parameterizations used in the simulation codes are largely based on theory and observations over flat terrain.

This paper investigates the steps necessary to achieve accurate simulations of the wind and temperature fields in the Riviera Valley, located in the Alps in southern Switzerland. As our simulation tool we use the Advanced Regional Prediction System (ARPS) (Xue et al., 2000, 2001). Intended mainly for mesoscale and small-scale atmospheric simulations, ARPS is formulated as an LES code and solves the three-dimensional, compressible, non-hydrostatic, filtered Navier-Stokes equations. Ultimately, the goal of this work is to accurately simulate, using all available data, the physical processes in this complex valley region and to improve understanding of valley flow physics. This work focuses on the numerical aspects of the large-eddy simulation needed to accurately represent the Riviera Valley flow. A companion paper (Weigel et al., 2004b) describes the physical and meteorological features of our simulated valley flows.

The Riviera Valley is a medium-sized valley located in the province of Ticino in southern Switzerland. The valley is on a highly-trafficked route; of interest, therefore, are the transitions of slope and along-valley winds, and the vertical structure of the atmosphere which determine mixing and transport of near-surface pollutants. The valley was the focus of an extensive field campaign, the MAP-Riviera Project (Rotach et al., 2004), yielding a relatively large number of field measurements useful for detailed comparison to numerical simulations.

Simulations of the Riviera Valley are complicated by the complex terrain, the low resolution of regional datasets available for initialization, and numerical discretization and lateral boundary condition errors, among other issues. Many studies over complex terrain point to increased grid resolution as a means to achieving

better agreement of simulations with observations (see e.g. Gronas and Sandvik (1999); Grell et al. (2000)). Hanna and Yang (2001) suggest that errors in wind speeds and directions in their simulations (using four different mesoscale codes) were due to errors in the representation of turbulent motions, as well as to subgrid features in the topography and land use. Zhong and Fast (2003) performed simulations of the Salt Lake Valley region using three mesoscale models at down to 560 m resolution, but relatively large forecast errors still existed despite the increased resolution. Likewise, despite using resolutions as high as 267 m in the horizontal, Gohm et al. (2004) found significant discrepancies between the simulations and the observations in the Rhine Valley.

Simulations of the Riviera Valley were performed by De Wekker et al. (2004) using the RAMS model and a two-way grid nesting approach with grid spacings down to 333 m. The results showed relatively good agreement with field observations for the potential temperature fields. However, the numerical model was not able to capture the wind structure of the valley very well; a consistent structure of up-slope and up-valley winds was not apparent. Our simulation setup has many similarities to that of De Wekker et al. (2004), as discussed further below.

Several steps have been taken in our work to address the numerical challenges present in this complex flow; the numerical setup and grid nesting approach which lead to the most accurate results are described in detail below. We then present sensitivity tests with a focus on the effects of soil moisture (which was found to have the largest impact) and topographic shading (as it has not been previously studied elsewhere). The effects of land use data, grid resolution, and turbulence closure models have also been examined; the results will appear in our future work, and can also be seen in Chow (2004).

2. NUMERICAL SIMULATION SETUP

The steps we have taken include the careful choice of grid nesting parameters, high-resolution surface data, and modifications to the radiation model. These steps are presented in contrast to the standard "acceptable" procedure using grid nesting, the standard initial conditions and surface datasets. Table 1 lists the simulations performed with various configurations; more details are given later.

2.1 Grid nesting and topography

Five one-way nested grids were used to simulate flow conditions in the Riviera Valley at horizontal resolutions of 9 km, 3 km, 1 km, 350 m, and 150 m (see Table 2 and Fig. 1). While the Riviera Valley is already visible on the 1km grid, its fine structure and tributaries first become reasonably well-resolved at 350 m resolution. Topography

* *Corresponding author address:* Environmental Fluid Mechanics Laboratory, Department of Civil and Environmental Engineering, Stanford University, Terman Engineering Center M-13, Stanford, CA 94305-4020, email: katopodes @ stanfordalumni.org

Table 1: Simulation configurations.

Run name	Configuration
REF	reference simulation set, simple grid nesting with no additional data
MOISLU	1 km grid: elevation-dependent soil moisture, 350 m grid: WaSiM soil moisture and 30 m land use data
MOISLU-NS	same as MOISLU but with no topographic shading for all grids
MOISLU2	1 km grid: WaSiM soil moisture, 350 m grid: WaSiM soil moisture and 30 m land use data

Table 2: Simulation parameters for each grid level.

(nx,ny,nz)	Δh	$\Delta z_{min}, \Delta z_{avg}$	$\Delta t, \Delta \tau$
(103,103,53)	9 km	50 m, 500 m	10 s, 10 s
(103,103,53)	3 km	50 m, 500 m	2 s, 4 s
(99,99,63)	1 km	50 m, 400 m	1 s, 1 s
(83,83,63)	350 m	30 m, 350 m	1 s, 0.2 s
(83,99,83)	150 m	20 m, 200 m	0.5 s, 0.05 s

for the 9 km through 1 km grids was obtained using the USGS 30 arc second topography datasets. For the 350 m and 150 m resolution simulations, the topography was extracted from a 100 m dataset available for Switzerland (Volkert, 1990). For each nested subdomain the terrain is smoothed near the domain boundaries to match the elevations from the surrounding coarser grid. ARPS uses a terrain following σ -coordinate system; the minimum vertical grid spacing (Δz_{min}) at the surface, as well as the average spacing (Δz_{avg}), are listed in Table 2. The domain height (~ 25 km) goes beyond the tropopause. ARPS uses large (Δt) and small ($\Delta \tau$) time steps in a mode-splitting scheme. The horizontal spacing (Δh) is uniform in both directions.

2.2 Initialization and lateral boundary conditions

To obtain realistic initial and boundary conditions, analysis data from the European Centre for Medium-Range Weather Forecasts (ECMWF) (50 vertical levels and 0.5 degree horizontal resolution) were used to force ARPS simulations at the 9 km grid. Lateral boundary condition forcing was applied at six-hour intervals and linearly interpolated in between. Relaxation towards the lateral boundary values was applied for a 5-10 grid-cell zone around the edge of the domain. Simulations were then performed for 30 hours beginning at 1800 UTC August 24; output was stored at hourly intervals and used to generate initial and boundary condition files for subsequent nested grid simulations.

The ECMWF initialization data provide a reasonable representation of synoptic conditions as compared to nearby sounding profiles. The simulation period of August 25, 1999 included a pronounced inversion observed at 2 km ASL. While the ECMWF data used for initialization incorporate observation data, the vertical resolution does not entirely capture this fine vertical feature.

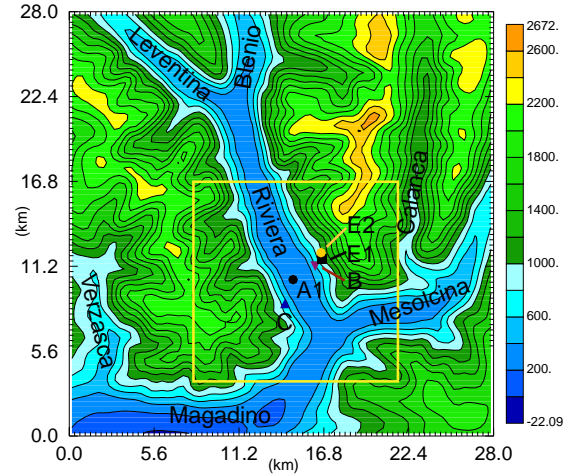
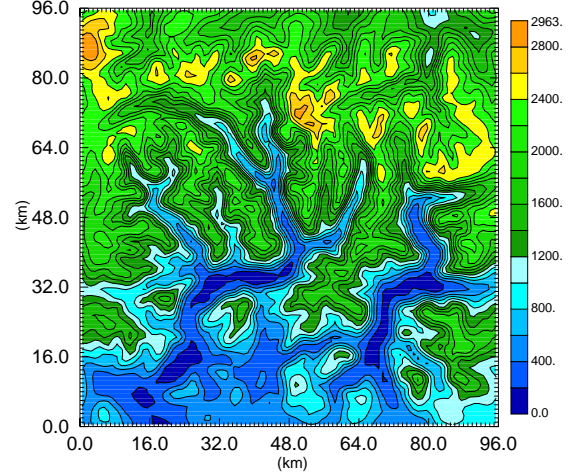


Figure 1: Riviera Valley elevation (m ASL) contours for (top) 1 km grid and (bottom) 350 m grid with the 150 m grid shown within.

2.3 Surface characteristics

ARPS normally uses 13 soil types (including water and ice), and 14 vegetation type classes. ARPS was modified to incorporate land use data from USGS 30 second global data for the 1 km (and coarser) grids. For the higher resolution grids (350 m and finer), we have modified the ARPS surface data classes to incorporate a dataset at 100 m resolution (from the Landnutzungskarte des Bundesamts für Statistik and the Digitale Bodeneignungskarte der Schweiz - GEOSTAT). The dataset includes 69 land use categories, which have been mapped to a new set of 30 vegetation and 14 soil types in ARPS (see Chow, 2004) as done by De Wekker (2002) for RAMS. Different values, however, have been chosen for the roughness length, leaf area index and vegetation fraction. A new soil type was added to represent bare rock, which makes up a significant portion of the mountain tops.

Soil temperature for all grids was specified as a constant offset (based on field measurements) from the near-surface air temperature (0.6 K for the top layer, -2.1 K for the deep soil, at the model initialization time).

Table 3: Typical soil moisture values (m^3m^{-3}) for each dataset in the surface and deep layers. All have close to zero soil moisture at the rocky outcroppings. The 3-level data are constant in each elevation range.

	Surface (0.01 m)	Deep (1.0 m)	
		Valley floor	Slopes
ECMWF	0.35	0.366	0.366
WaSiM	0.32	0.25	0.08-0.12
3-level	same as deep	0.28	0.18

Soil moisture for the 9 km resolution grid was initialized using values from the ECMWF dataset; typical values are given in Table 3. These are then interpolated to the 3 km resolution grid, and for the REF simulations (see Table 1), further interpolated to the 1 km and 350 m grids.

To better represent the spatial variability in the Riviera Valley, the MOISLU and other simulations follow the approach of De Wekker et al. (2004), using the Water Flow and Balance Simulation Model (WaSiM-ETH) (Jasper, 2001) to obtain higher resolution soil moisture information. The hydrologic model is driven by meteorological data such as air temperature and precipitation and provided 100 m resolution data for the catchment region of the Riviera. The WaSiM data compare well with the few observation points available in the Riviera.

Given the ECMWF data at the coarsest grid, and the WaSiM data at the finest grids, the question remains as to what the best soil moisture values are at the intermediate resolutions of 3 km and 1 km. De Wekker et al. (2004) set the soil moisture constant on the coarser grids and found that the specific value did not significantly affect the results. Our sensitivity studies (see Section 5), however, show that soil moisture is one of the most sensitive parameters in these simulations. We have therefore incorporated a semi-empirical three-level soil moisture initialization at the 1 km level, used in the MOISLU simulations. These values provide an intermediate (height-dependent) value for both soil model levels and can be seen as a compromise between the WaSiM and ECMWF data (see Table 3).

2.4 Incoming radiation model

ARPS normally includes the effect of surface inclination when calculating incoming solar radiation. Colette et al. (2003) found that the inclusion of topographic shading (the shadow cast by neighboring topography) could delay inversion layer breakup during the morning by up to half an hour in idealized simulations of steep valleys. The field study of Matzinger et al. (2003) emphasized the importance of the topographic shade in the Riviera Valley, where local sunrise is delayed with significant effects on the net radiation balance. To improve the treatment of radiation in our simulations of a real mountain valley, we have therefore included the topographic shading method of Colette et al. (2003) in our simulations. Its effect is evaluated in Section 5.2. This feature is now included in the latest version of ARPS.

2.5 Turbulence and computational mixing

The standard 1.5-order TKE closure model is used

to represent turbulent mixing (Deardorff, 1980; Moeng, 1984). The use of the TKE model is admissible in an LES context as long as the chosen length scale is proportional to the filter width, as it is in ARPS (Deardorff, 1980; Moeng, 1984). The TKE approach is especially useful when a large fraction of the velocity scales are contained in the subfilter scales as with coarse resolution grids (Pope, 2000, Chapter 13). New subfilter-scale (SFS) turbulence closure methods have also been applied, but results are not presented here (see Chow (2004)).

Fourth-order computational mixing is used to damp high frequency motions that can build up due to nonlinear interactions. ARPS also includes a divergence damping term to control acoustic noise. The impact of both of these damping terms has been investigated and the coefficients were set to give the minimum amount of mixing required for stability.

3. MEAN WIND PATTERNS

Typical thermally-driven valley wind patterns include the onset of up-slope winds in the morning, followed by up-valley winds during the day. In the evening, the winds transition to down-slope and down-valley winds (Whiteman, 2000). Slope winds are generated by differential heating of air near the surface along the slopes, and air in the middle of the valley. A pressure gradient results, which during the day drives the lighter, warmer air up the slope, and at night drives the heavier, cooler air down the slope. The mechanism for along-valley winds is not as simply explained, but can perhaps in part be understood by the “topographic amplification factor” (Steinacker, 1984; McKee and O’Neal, 1989).

The winds in the Riviera exhibit some of these typical patterns as well. Figure 2 shows the evolution of potential temperature, and surface wind speed and direction at Bosco di Sotto (site A1, see Fig. 1) near the center (46.2547 N, 9.0117 E) of the simulation domains, compared to results from the REF and MOISLU simulations. All results are from the 350 m resolution grid unless otherwise noted. The 150 m simulations are used to extract heat and moisture fluxes used in the companion paper (Weigel et al., 2004b). During the first 6-7 hours on August 25, 1999, the predominant winds in the valley are down-valley at about 330° . Between 0600 and 0800 UTC (CET local daylight savings time = UTC + 2 hours), winds shift to up-valley at about 150° . Local sunrise is at approximately 0700 UTC at the valley floor, but is earlier on the east-facing slopes and in the Magadino Valley. Sunset is at approximately 1600 UTC, and the winds shift to down-valley by about 1800 UTC. The surface winds are generally weak during the night and become strong during the day with the onset of the up-valley flow.

The MOISLU simulation results in the wind speed comparisons in Figs. 2b and c show a 1-2 hour delay in the onset of the up-valley winds compared to the observations at 28 m AGL at Bosco di Sotto. This is significantly improved from the REF simulations, however, where the delay evident in the wind speed is 3-4 hours. The wind direction recorded when the wind speed is weak fluctuates a lot, making comparisons with model results difficult. Nevertheless, the potential temperature, and surface wind direction and speed are quite well reproduced by the MOISLU results. The results of De Wekker et al. (2004) showed a 2 hour delay in the onset of the up-valley winds and were also not able to capture the evening transition to

Table 4: Root-mean-square errors and mean errors (bias) for potential temperature (θ), wind speed (U), and wind direction (ϕ), for simulations compared to observations at Bosco di Sotto (site A1), using average of 15.9 and 28 m values, and at three sites on the eastern slope (sites B, E1 and E2), using data from a variety of measurement heights.

	Site A		Sites B, E1, E2	
	REF	MOISLU	REF	MOISLU
θ rmse (K)	3.20	0.86	1.12	0.85
θ bias (K)	-3.04	-0.51	-0.53	0.03
U rmse (m/s)	1.47	1.20	1.13	1.19
U bias (m/s)	-0.53	0.41	-0.35	0.12
ϕ rmse (deg)	86.42	65.01	71.13	65.96
ϕ bias (deg)	-1.50	-15.89	-1.97	-8.19

down-valley winds. The most likely reason for the delays in the ARPS simulations is poor representation of surface soil conditions; the soil moisture and temperature control the heating and cooling of the surface, thus controlling the strength of along valley and slope winds. Sensitivity tests in Section 5.1 show that changes in the soil moisture can significantly change the onset of valley wind transitions. The sensitivity to the soil temperature was not as large, and was not investigated further.

Comparisons to wind observations at surface stations at Pian Perdascio (site C, east-facing slope) and Monte Nuovo (site E2, west-facing slope) (see Fig. 1), also show quite good agreement for the MOISLU simulations, in particular for the wind speeds (not shown). These comparisons along the slopes can be very sensitive to the exact location chosen, as moving 100 m to the right or left can also mean an elevation change of almost 100 m.

A more quantitative comparison can be obtained by examining the magnitude of errors between the observations and the simulation results. Table 4 shows the root-mean-square errors (rmse) and mean errors (bias) for wind speed and direction and potential temperature comparisons at surface station A1, as well as a composite of the errors at three sites on the eastern slope (sites B, E1 and E2). The bias provides an indication of the average direction of deviation of the modeled from the observed data, whereas the rmse provides an estimate of the magnitude of the error. The errors are overall quite small (e.g. less than 1 K for potential temperature), especially when compared to the results of other typical simulations. The MOISLU results significantly reduce the errors in all comparisons except the wind direction bias, where the REF results exhibited more fluctuations and hence a lower overall bias.

4. BOUNDARY LAYER EVOLUTION

In addition to the along-valley wind transitions visible at surface stations, the vertical structure of the atmosphere, as measured in radio soundings, reflects important features of the flow. Figure 3 shows comparisons of the REF and MOISLU simulation results for potential temperature, wind speed, wind direction, and specific humidity, to radio sounding data obtained at Bosco di Sotto (station A1) at a few selected times. The morning atmosphere (0739 UTC, not shown) is characterized by a stable layer in the

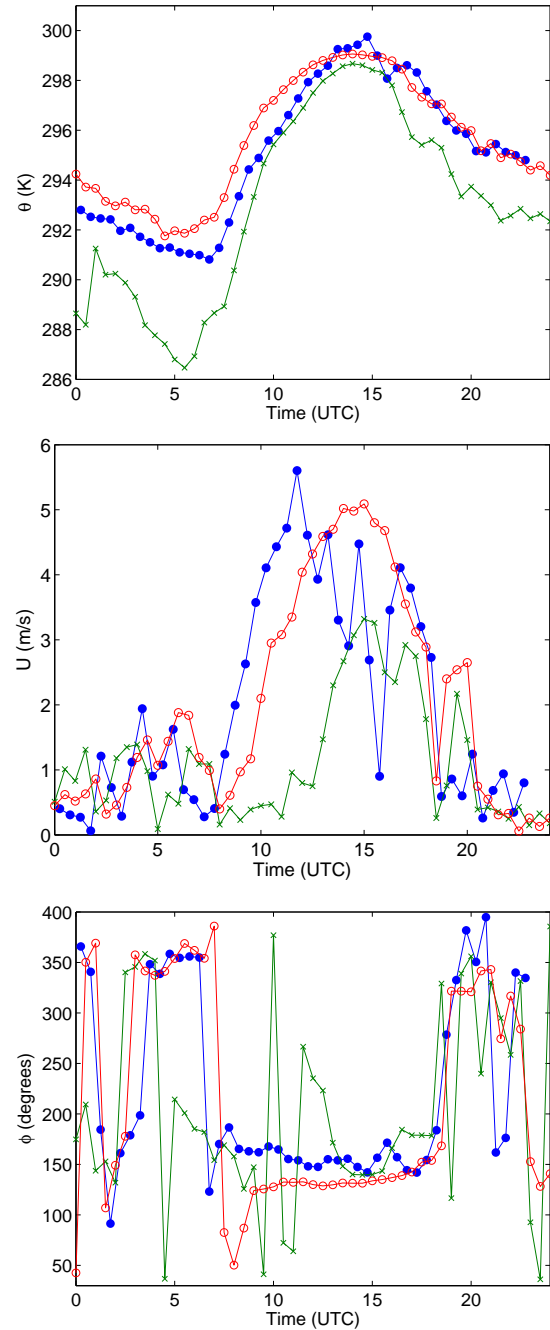


Figure 2: Surface data time series comparisons at Bosco di Sotto (site A1, valley floor) for (a) potential temperature, (b) wind speed and (c) wind direction. —●— Observations at 28 m AGL; —○— MOISLU; —x— REF

Table 5: Root-mean-square errors and mean errors (bias) for potential temperature (θ), wind speed (U), wind direction (ϕ), and specific humidity (q), for all radio sounding launches for MOISLU and REF simulations.

	REF	MOISLU
θ rmse (K)	1.43	1.00
θ bias (K)	-0.73	-0.28
U rmse (m/s)	2.29	2.07
U bias (m/s)	-0.35	-0.16
ϕ rmse (deg)	55.47	47.55
ϕ bias (deg)	3.96	-5.79
q rmse (g/kg)	1.45	1.13
q bias (g/kg)	-0.75	-0.22

bottom 1.5 km ASL, a very stable layer until 2.2 km ASL, and a mixed or slightly stable layer above that extending to about 4.5 km ASL.

Typical valley inversion layer breakup theory predicts that a mixed layer will grow at the surface as long as there is surface heating, as on such a “convective” day. Most interesting in this context is that the mixed layer in the Riviera stops growing in the late morning despite positive surface heat fluxes. This phenomenon is further discussed in Weigel and Rotach (2004) and in our companion paper (Weigel et al., 2004b).

The agreement of the MOISLU results with the sounding profiles in Fig. 3 is excellent, especially when compared to the REF results which do not perform very well near the ground. In particular, the REF simulations do not develop a mixed layer near the ground evident in the observations at 0915 UTC; the wind direction predicted by REF also fails to exhibit the observed up-valley flow at 0915 and even does not do well at 1208 UTC near the surface. Both simulations underpredict the observed surface warming during the afternoon. The wind speed profiles are especially difficult to compare because of the fluctuations captured in the sounding data, as well as the very heterogeneous flow structure in the valley (see Weigel and Rotach, 2004). We cannot expect the LES results to provide exactly the same instantaneous profiles, but rather to represent the “mean” or resolved-scale structure.

Table 5 compares the overall rmse and bias for all sounding times for the MOISLU and REF simulations, including data up to 6 km ASL. The errors are quite small (e.g. ~ 2 m/s for wind speed) and confirm the good agreement of the results with the observations seen visually.

5. SENSITIVITY TESTS

The comparisons in Sections 3 and 4 contrasted the best results (MOISLU) with those from the standard “acceptable” procedure using the standard initial conditions and surface datasets (REF). The results show high sensitivity to surface data. We now discuss the separate effects of soil moisture and topographic shading.

5.1 Soil moisture

The improvement resulting from the use of high-resolution soil moisture data from WaSiM has already

been shown in Figs. 2-3 by comparing the REF and MOISLU simulations. The REF simulations used soil moisture data from ECMWF datasets; the result is that the up-valley wind transition occurs too late (by 3-4 hours) throughout the entire nesting set. The soil moisture clearly has a strong effect on the development of valley winds (via latent heat fluxes, see e.g. (Banta and Gannon, 1995; Ookouchi et al., 1984)). Tests indicate that the difference is largely due to the soil moisture used at the 1 km nesting level (Weigel et al., 2004a).

Lacking any high resolution data for the 1 km grid, we explored three different approaches for initializing the soil moisture at this nesting level, as previously described (see Table 3). The improvements due to using WaSiM data in the MOISLU simulations motivated an attempt to use the WaSiM data at the coarse resolutions as well. The WaSiM data, however, covers only the Ticino and Verzasca river catchment areas, i.e. only the immediate vicinity of the Riviera. We therefore apply the WaSiM data at the 1 km grid level (MOISLU2 simulations) where data are available; over the rest of the domain we use elevation-dependent values at three levels (similar to the MOISLU setup) determined from averages of the WaSiM data. Thus we extrapolate the values from the center of the domain, where the WaSiM data are available, to the rest of the Alps region at the 1 km grid level. Figure 4 shows a comparison of the MOISLU and MOISLU2 wind speed, which unfortunately shows an increased delay in the onset of the valley winds and that the up-valley winds die out too soon in the evening.

The results from MOISLU, MOISLU2 and REF indicate that the values of the soil moisture outside the fine-grid domain are crucial for accurately predicting the wind transitions. We find that the simulations deteriorate in quality if we assume a large scale soil moisture distribution (ECMWF) to also hold on the regional scale (1km domain). Likewise, assuming that the local soil moisture distribution (WaSiM) in the Riviera Valley also holds over a larger (1km) domain, also yields poorer results. This points to the need for high-resolution soil moisture measurements over a broader region (such as the Alps) to provide accurate input to the large-eddy simulations.

5.2 Topographic shading

Figure 5 shows the surface radiation balance at surface station A1. The model slightly overpredicts the incoming shortwave radiation during the day. The peak of the curve is highly sensitive to its spatial location and could be adjusted by improving the spatial interpolation from the simulation results. The magnitude of the net radiation is underpredicted, mostly at night. This may be due to the fact that the radiation model does not take into account the incoming longwave emissions from the valley walls throughout the night.

Zhong and Fast (2003) suggest that the absence of topographic shading in their simulations caused discrepancies. Figure 6 shows the incoming shortwave radiation obtained with and without topographic shading. The incoming shortwave radiation is significantly reduced during sunrise and sunset when topographic shading is included, and therefore compares better with the measurements. Figure 7 shows the spatial variation in the difference in incoming shortwave radiation at 0600 UTC when topographic shading is included. The east-facing slopes are shaded while the sun is low on the horizon, resulting

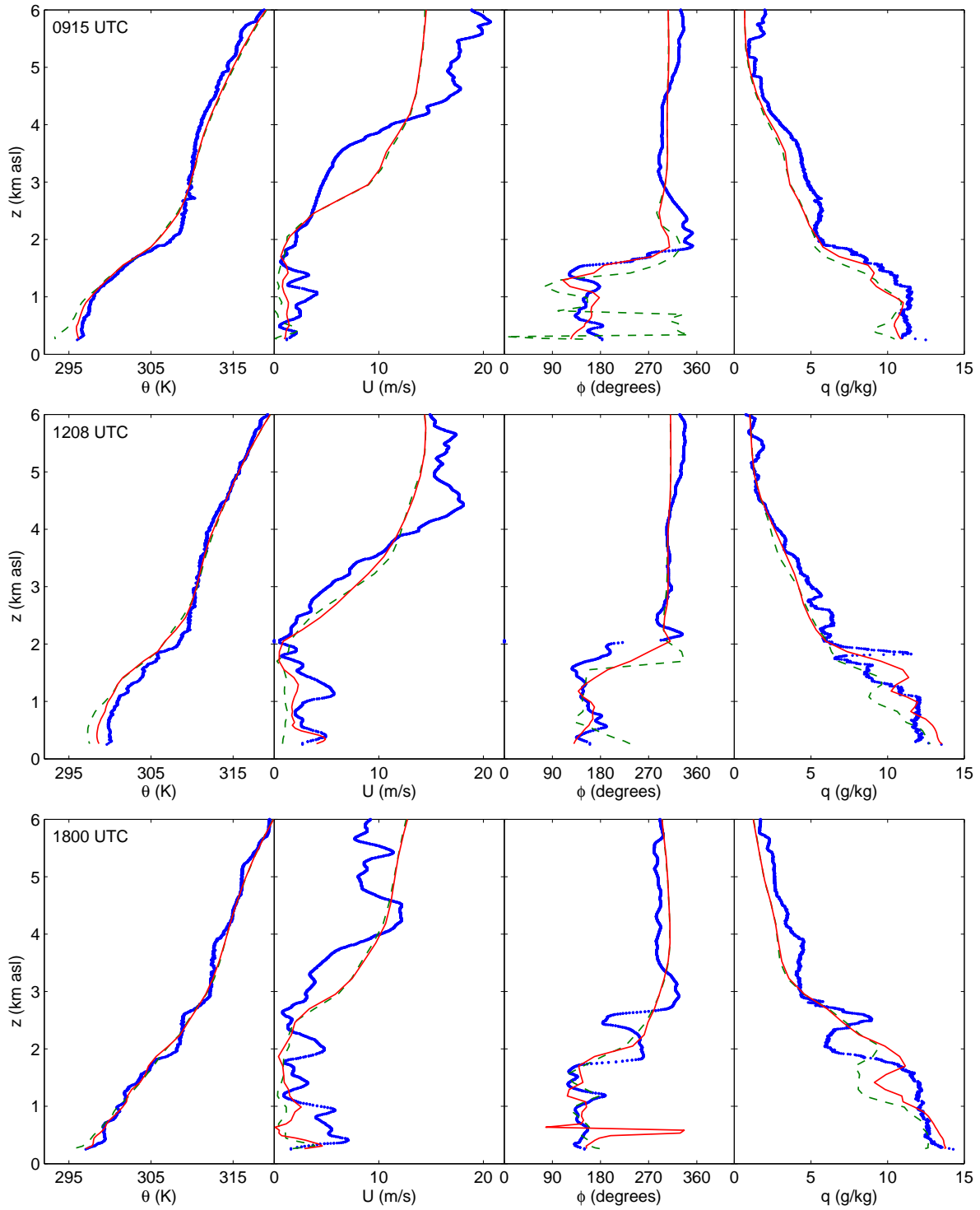


Figure 3: Radio soundings at Bosco di Sotto (site A1) of potential temperature, wind speed, wind direction, and specific humidity at 0915, 1208, and 1800 UTC. — Observations; — MOISLU; - - REF

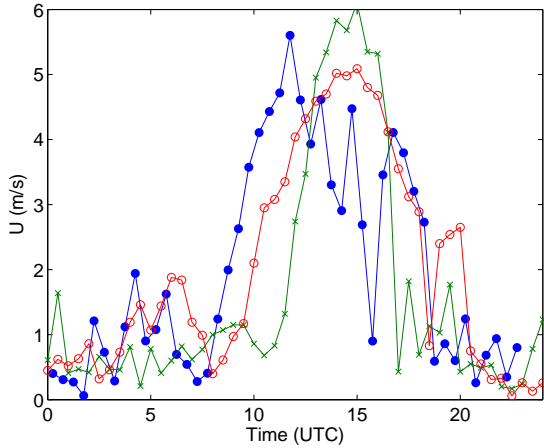


Figure 4: Surface wind speed at Bosco di Sotto (site A1).
 —●— Observations; —○— MOISLU; —×— MOISLU2

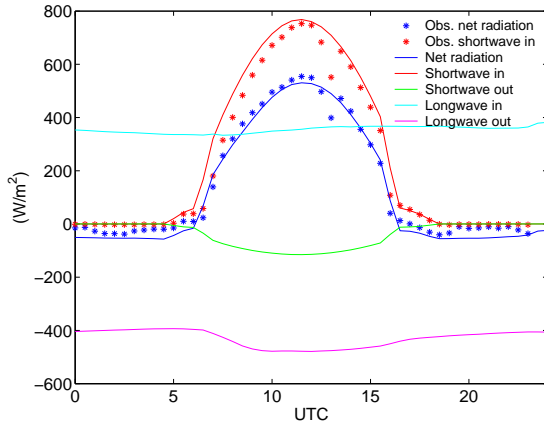


Figure 5: Radiation budget components compared to observations at site A1.

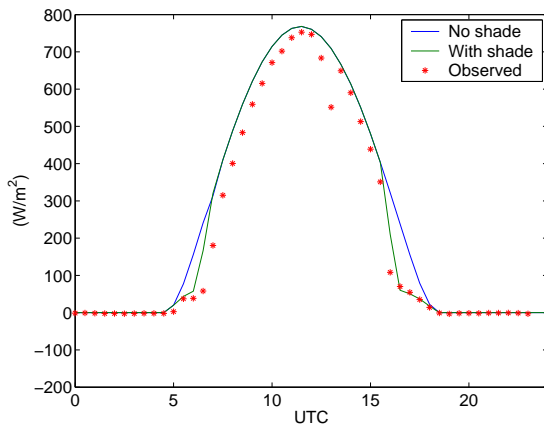


Figure 6: Incoming solar radiation, with and without topographic shading at site A1.

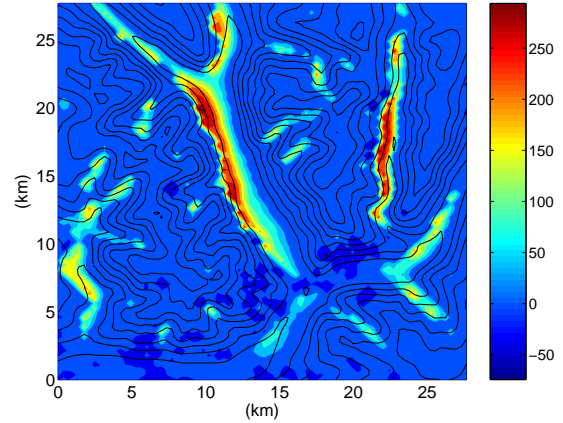


Figure 7: Difference in shortwave incoming radiation (shaded, W/m^2) with and without shading for the 350 m grid at 0600 UTC. Elevation contours (lines) shown at 250 m intervals.

in differences close to $300 W/m^2$.

A series of simulations was performed without topographic shading for the entire set of simulations (MOISLU-NS). The difference in the results is insignificant at the coarser resolutions, as the slopes of the topography are smaller. At the 350 m grid level, surface temperatures are slightly warmer without shading ($\sim 0.5-1.0 K$) during sunrise and sunset, as expected. The resulting influence of the topographic shading in the radio sounding comparisons is small, however. The MOISLU-NS simulations also show increased up-slope winds along the east-facing slope of the Riviera during sunrise; however, the difference is only on the order of 0.1 m/s (occasionally up to 0.5 m/s).

Larger differences were observed in the idealized simulations of Colette et al. (2003), where along-valley winds were absent. The strong along-valley winds quickly overwhelm the influence of slight differences in the up-slope winds in the Riviera. Another reason why the impact of topographic shading may not be as strong may be that the valley winds originate in the Magadino and Leventina Valleys (to the south and north of the Riviera, respectively). These valleys have more of an east-west orientation and are thus less affected by topographic shading in the morning. While the differences between the MOISLU and MOISLU-NS simulations are apparently small, the improvement in the radiation curves in Fig. 6 is significant. The computational cost of the subroutine is negligible (Colette et al., 2003); therefore we include the topographic shading in our simulations.

6. CONCLUSIONS

We have shown that ARPS is able to accurately reproduce the valley wind transitions and vertical structure observed under convective conditions during the MAP-Riviera project field campaign of 1999. This requires careful initialization with high-resolution land use and soil moisture data sets, among other considerations. In contrast, a straightforward grid nesting approach does not yield satisfactory results. The sensitivity of the results

to changes in simulation settings is explored by comparisons to radio soundings and surface measurements on the Riviera Valley floor. It is found that even with strong local thermal forcing, the onset and magnitude of the up-valley winds are highly sensitive to surface fluxes in areas which are well outside the high-resolution domain. These processes are inadequately resolved on the coarser grid of the previous nesting level, and directly influence the flow structure in the high-resolution domain via its lateral boundary conditions. While the impact of topographic shading on the flow dynamics is small, the improvement in the radiation curves is significant. The sensitivity to surface conditions (particularly soil moisture) points to the need for better surface observation measurements and datasets for initialization.

6. ACKNOWLEDGMENTS

The support of a National Defense Science and Engineering Graduate fellowship [FKC], NSF Grants ATM-0073395 (Physical Meteorology Program: W.A. Cooper, Program Director) [FKC and RLS], ATM-9909007 and 0129892 [MX], and the Swiss National Science Foundation (Grants #20-68320.01 and #20-100013) [APW], are gratefully acknowledged. Acknowledgment is also made to the National Center for Atmospheric Research, which is sponsored by NSF, for the computing time used in this research.

REFERENCES

- Banta, R. M. and P. T. Gannon, 1995: Influence of soil moisture on simulations of katabatic flow. *Theoretical and Applied Climatology*, **52**, 85 – 94.
- Chow, F., 2004: *Subfilter-scale turbulence modeling for large-eddy simulation of the atmospheric boundary layer over complex terrain*. Ph.D. dissertation, Stanford University.
- Colette, A., F. K. Chow, and R. L. Street, 2003: A numerical study of inversion-layer breakup and the effects of topographic shading in idealized valleys. *Journal of Applied Meteorology*, **42**, 1255 – 1272.
- De Wekker, S., 2002: *Structure and morphology of the convective boundary layer in mountainous terrain*. Ph.D. dissertation, University of British Columbia.
- De Wekker, S., D. G. Steyn, J. D. Fast, M. W. Rotach, and S. Zhong, 2004: The performance of RAMS in representing the convective boundary layer structure in a very steep valley. *Environmental Fluid Mechanics*, **in press**.
- Deardorff, J. W., 1980: Stratocumulus-capped mixed layers derived from a 3-dimensional model. *Boundary-Layer Meteorology*, **18**, 495 – 527.
- Gohm, A., G. Zängl, and G. J. Mayr, 2004: South foehn in the Wipp Valley on 24 October 1999 (MAP IOP 10): Verification of high-resolution numerical simulations with observations. *Monthly Weather Review*, **132**, 78 – 102.
- Grell, G. A., S. Emeis, W. R. Stockwell, T. Schoenemeyer, R. Forkel, J. Michalakes, R. Knoche, and W. Seidl, 2000: Application of a multiscale, coupled MM5/chemistry model to the complex terrain of the VOTALP valley campaign. *Atmospheric Environment*, **34**, 1435 – 1453.
- Gronas, S. and A. D. Sandvik, 1999: Numerical simulations of local winds over steep orography in the storm over north Norway on October 12, 1996. *Journal of Geophysical Research*, **104**, 9107–20.
- Hanna, S. R. and R. X. Yang, 2001: Evaluations of mesoscale models' simulations of near-surface winds, temperature gradients, and mixing depths. *Journal of Applied Meteorology*, **40**, 1095 – 104.
- Jasper, K., 2001: *Hydrological modelling of Alpine river catchments using output variables from atmospheric models*. Ph.D. dissertation, ETH No. 14385, Swiss Federal Institute of Technology, Zurich.
- Matzinger, N., M. Andretta, E. V. Gorsel, R. Vogt, A. Ohmura, and M. W. Rotach, 2003: Surface radiation budget in an alpine valley. *Quarterly Journal of the Royal Meteorological Society*, **129**, 877 – 895.
- McKee, T. B. and R. D. O'Neal, 1989: The role of valley geometry and energy budget in the formation of nocturnal valley winds. *Journal of Applied Meteorology*, **28**, 445 – 56.
- Moeng, C.-H., 1984: A large-eddy-simulation model for the study of planetary boundary-layer turbulence. *Journal of Atmospheric Sciences*, **41**, 2052–2062.
- Ookouchi, Y., M. Segal, R. C. Kessler, and R. A. Pielke, 1984: Evaluation of soil moisture effects on the generation and modification of mesoscale circulations. *Monthly Weather Review*, **112**, 2281 – 92.
- Pope, S. B., 2000: *Turbulent flows*. Cambridge University Press, Cambridge, UK, 770 pp.
- Rotach, M. W. et al., 2004: Turbulence structure and exchange processes in an Alpine valley: The Riviera project. *Bulletin of the American Meteorological Society*, **in press**.
- Steinacker, R., 1984: Area-height distribution of a valley and its relation to the valley wind. *Contributions to Atmospheric Physics*, **57**, 64 – 71.
- Volkert, H., 1990: An alpine orography resolving major valleys and massifs. *Meteorology and Atmospheric Physics*, **43**, 231 – 4.
- Weigel, A. P., F. K. Chow, M. W. Rotach, and R. L. Street: 2004a, Assessment of large-eddy simulations of the atmospheric boundary layer in a steep and narrow Alpine valley. *Geophysical Research Abstracts*, European Geosciences Union First General Assembly, Nice, France, volume 6, EGU04–A–03496.
- Weigel, A. P., F. K. Chow, M. W. Rotach, R. L. Street, and M. Xue: 2004b, High-resolution large-eddy simulations of the riviera valley: assessment of the flow structure and the heat and moisture budgets. *11th Conference on Mountain Meteorology*, American Meteorological Society.
- Weigel, A. P. and M. W. Rotach, 2004: Flow structure and turbulence characteristics of the daytime atmosphere in a steep and narrow alpine valley. *Quarterly Journal of the Royal Meteorological Society*, **in press**.
- Whiteman, C. D., 2000: *Mountain meteorology: fundamentals and applications*. Oxford University Press, 355 pp.
- Xue, M., K. K. Droegemeier, and V. Wong, 2000: The advanced regional prediction system (ARPS): A multi-scale nonhydrostatic atmospheric simulation and prediction model. Part I: Model dynamics and verification. *Meteorology and Atmospheric Physics*, **75**, 161–193.
- Xue, M., K. K. Droegemeier, V. Wong, A. Shapiro, K. Brewster, F. Carr, D. Weber, Y. Liu, and D. Wang, 2001: The advanced regional prediction system (ARPS): A multi-scale nonhydrostatic atmospheric simulation and prediction tool. Part II: Model physics and applications. *Meteorology And Atmospheric Physics*, **76**, 143–165.
- Zhong, S. Y. and J. Fast, 2003: An evaluation of the MM5, RAMS, and Meso-Eta models at subkilometer resolution using VTMX field campaign data in the Salt Lake Valley. *Monthly Weather Review*, **131**, 1301 – 1322.